Korean J. Chem. Eng., **27**(3), 822-827 (2010)
DOI: 10.1007/s11814-010-0126-6

The effect of cobalt precursors on NO oxidation over supported cobalt oxide catalysts

Dae Su Kim*, Yun Ha Kim*, Jae Eui Yie, and Eun Duck Park*,†**

*Division of Energy Systems Research and Division of Chemical Engineering and Materials Engineering,
**Division of Applied Biotechnology,
Ajou University, San 5 Wonchun-dong, Yeongtong-gu, Suwon 443-749 Korea
(*Received 27 August 2009 • accepted 25 September 2009*)

Abstract−The effect of cobalt precursors such as cobalt acetate and cobalt nitrate on NO oxidation was examined over cobalt oxides supported on various supports such as SiO_2, ZrO_2, and CeO_2. The N_2 physisorption, X-ray diffraction (XRD), transmission electron microscopy (TEM), temperature-programmed reduction with H_2 (H_2-TPR), NO chemisorptions, and temperature-programmed oxidation (TPO) with mass spectroscopy were conducted to characterize catalysts. The NO uptake as well as the catalytic activity for NO oxidation was dependent on the kinds of cobalt precursors and supports for supported cobalt oxides catalysts. Among tested catalysts, Co_3O_4/CeO_2 prepared from cobalt acetate showed the highest catalytic activity. The catalytic activity generally increased with the amount of chemisorbed NO. Reversible deactivation was observed over Co_3O_4/CeO_2 in the presence of H_2O. On the other hand, irreversible deactivation occurred over the same catalyst even in the presence of 5 ppm SO_2 in a feed. The strongly adsorbed SO_2 can prohibit NO from adsorbing on the active sites and also can prevent formed NO_2 from desorbing off the catalyst surface. The formation of SO_3 cannot be observed from the chemisorbed SO_2 on Co_3O_4/CeO_2 during TPO.

Key words: NO Oxidation, Co_3O_4, Precursors, SO_2, H_2O

INTRODUCTION

Nitrogen oxides (NO_x) such as NO and NO_2 have been generated from high-temperature oxidation processes in the presence of N_2 or the combustion of N-containing fuels. Because of their adverse characteristics causing acid rain, a photochemical smog, an ozone layer destruction, and a green house effect [1], various methods for NO_x control have been examined such as the selective catalytic reduction (SCR), NO_x storage and reduction (NSR) and the selective NO_x recirculation (SNR) [1-5]. Among them, the SCR has been regarded as the representative way to decrease NO_x concentration in the flue gas. The reaction rate for SCR with NH_3 as a reducing agent (NH_3-SCR) has been reported to be directly dependent on the fraction of NO_2 in NO_x [6-10]. The enhancement in the de-NO_x rate can be noticeable especially at low temperatures such as 200-300 °C when the equimolar amounts of NO and NO_2 are present in a feed (fast SCR process). This beneficial effect on SCR in the presence of NO_2 has also been reported for the SCR of NO with hydrocarbons [11-18].

In the lean burning natural gas or diesel engine, NO_x is mainly composed of NO. Therefore, the oxidation of NO into NO_2 can be an important reaction for NO_x control. Until now, several catalyst systems have been examined for NO oxidation. They can be grouped into the noble metals [19-33] and the transition metal oxides [34-47] catalysts. Among noble metal catalysts, supported Pt-based catalysts have been intensively examined [20-32]. Compared with the noble metal catalysts, transition metal oxides have many advantages such as their low price and catalytic stability. As transition metal oxides, various catalyst systems have been examined such as CuO/SiO_2-Al_2O_3 (-TiO_2, -ZrO_2) [34], CuO/NiO/alumina [35], CuO/NiO/titania [35], Ag/Al_2O_3 [36], Ga-ZSM-5 [37], In-ZSM-5 [37], Fe-MFI [38,39], Fe-FER[38], Co/Al_2O_3 [40], Co-H-MFI [41], Co-H-FER [42], Co/TiO_2 [43], Co/ZrO_2 [43], Co/$K_xTi_2O_5$ [44,45] and Co_3O_4 [46]. Until now, Co-based catalyst systems have been frequently reported to have promising catalytic activity for NO oxidation. In the previous work [47], we found that the catalytic activity for NO oxidation is strongly dependent on the support. However, no relevant work on the effect of kinds of cobalt precursors on the catalytic activity for NO oxidation has yet been performed. In this study, cobalt oxides catalysts prepared from cobalt acetate and cobalt nitrate were compared for NO oxidation.

EXPERIMENTAL

1. Preparation of Catalysts

CeO_2 (Rhodia, S_{BET}=300 m^2/g) and SiO_2 (Aldrich, S_{BET}=348.7 m^2/g) were purchased and used as a support. Additionally, ZrO_2 was prepared with a precipitation method from $ZrOCl_2 \cdot 8H_2O$ (Junsei Chem.). 1 M NH_4OH solution was used as a precipitation agent and the precipitant was filtered, dried at 393 K and calcined in air at 773 K before use as a support. The BET surface area was determined to be 94 m^2/g for ZrO_2.

All the catalysts were prepared with a wet impregnation method from an aqueous solution of cobalt acetate ($Co(CH_3COO)_2 \cdot 4H_2O$, Junsei Chem.) or cobalt nitrate ($Co(NO_3)_2 \cdot 6H_2O$, Junsei Chem.). The cobalt oxide catalysts prepared from cobalt nitrate and cobalt acetate were denoted as Co_3O_4(N) and Co_3O_4(A), respectively. For example, the Co_3O_4(N)/CeO_2 containing 1.70 mmol $Co/g_{cat.}$ was prepared as follows. The aqueous solution of cobalt nitrate was prepared by dissolving 2.8 g of $Co(NO_3)_2 \cdot 6H_2O$ in 50 ml of the deionized water. 5.0 g of CeO_2 was put into the solution and mixed with

†To whom correspondence should be addressed.
E-mail: edpark@ajou.ac.kr

60 rpm in a rotary evaporator at an atmospheric pressure at 333 K for 6 h. The excess water was evaporated at 333 K in a vacuum condition and the impregnated sample was recovered and dried in an oven at 393 K for 12 h. The dried sample was calcined in air at 573 K before a reaction.

The cobalt oxide (Co_3O_4) was prepared as described in our previous work [47]. 1 wt% Pt/γ-Al_2O_3 was purchased from Aldrich and used as a reference catalyst. All the catalysts were calcined at 573 K in air for 1 h before a reaction.

2. Characterization of Catalysts

The BET surface area was calculated from N_2 adsorption data that were obtained using Autosorb-1 apparatus (Quantachrome) at liquid N_2 temperature. Before the measurement, the sample was degassed in vacuum for 4 h at 473 K.

Chemical composition of the prepared samples was analyzed by inductively coupled plasma-atomic emission spectroscopy (ICP-AES, JY-70Plus, Jobin-Yvon).

Bulk crystalline structures of catalysts were determined with an X-ray diffraction (XRD) technique. XRD patterns were recorded on a Rigaku D/MAC-III using Cu Kα radiation (λ=0.15406 nm), operated at 40 kV and 100 mA (4.0 kW). The crystalline size of Co_3O_4 was calculated by applying the Scherrer line broadening equation as follows [48].

$$L = \frac{0.9\lambda_{K_\alpha}}{B_{(2\theta)}\cos\theta_{max}}$$

where L denotes the average particle size, the value 0.9 is chosen when $B_{(2\theta)}$ is the full width at half maximum (FWHM) of the peak broadening in radians, λ_{K_α} is the wavelength of X-ray radiation (0.15406 nm), and θ_{max} is the angular position at the (311) peak maximum of Co_3O_4.

Temperature programmed reduction (TPR) was conducted in an AutoChem 2,910 unit (Micromeritics) equipped with a thermal conductivity detector (TCD) to measure H_2 consumption and an on-line mass spectrometer (QMS 200, Pfeiffer Vacuum) to detect any organic or inorganic species in the effluent stream during TPR experiment. A water trap composed of blue silica gel removed moisture from the TPR effluent stream at 273 K before the TCD. Quartz U-tube reactors were loaded with 0.10 g of sample except Co_3O_4. 10 mg of Co_3O_4 was loaded to obtain the accurate TPR pattern [49]. Catalysts were pretreated by calcinations in 20 vol% O_2 in N_2 at 573 K for 1 h, then cooled to room temperature. The TPR was performed by using 50 cm^3/min of 10 vol% H_2/Ar from 313 K to 1,173 K at a heating rate of 5 K/min and by monitoring the thermal conductive detector (TCD) signals after removing any residual oxygen in a line by flowing He at 313 K for 1 h.

NO uptake measurements were performed in an AutoChem 2,910 unit (Micromeritics) equipped with a thermal conductivity detector (TCD) to measure NO consumption and an on-line mass spectrometer (QMS 200, Pfeiffer Vacuum) to detect any organic or inorganic species in the effluent stream during NO uptake experiment. Quartz U-tube reactors were loaded with 0.1 g of sample. All the catalysts were pretreated by calcinations in 20 vol% O_2 in N_2 at 573 K for 1 h, then cooled to room temperature. The NO uptake measurement was carried out at 298 K in 30 cm^3/min of He stream through a pulsed-chemisorption technique, in which 500 ml pulses of NO were utilized, after removing any residual oxygen in a line by flowing He at 298 K for 1 h.

The temperature programmed oxidation (TPO) was carried out over Co_3O_4(A)/CeO_2 after NO oxidation in the presence of 100 ppm SO_2 in an AutoChem 2,910 unit (Micromeritics) and an on-line mass spectrometer (QMS 200, Pfeiffer Vacuum) to analyze the desorbed species in the effluent stream during TPO experiment. The TPO was performed by using 30 cm^3/min of 2 vol% O_2 in He from 313 K to 1,173 K at a heating rate of 10 K/min and by monitoring the mass signals after removing any residual species in a line by flowing He at 313 K for 1 h.

Bright-field images of transmission electron microscopy (TEM) were obtained using a Tecnai G^2 TEM (FEI) operated at 200 kV. Samples were ground in a mortar to fine particles and then dispersed ultrasonically in methanol. The sample was deposited on a Cu grid covered by a holey carbon film.

3. Activity Test

The catalytic activity was measured in a small fixed bed reactor of 8-mm i.d. with catalysts that had been retained between 45 and 80 mesh sieves. Reactant gases were fed to the reactor by means of electronic mass flow controller (MKS). The reactant gas typically consisted of 500 ppm NO and 5 vol% O_2 in N_2. All the lines were heated above 423 K to prevent any gas from condensation. The effect of water in a feed on the catalytic performance was examined under the feed composed of 500 ppm NO, 5 vol% O_2 and 5 vol% H_2O in N_2. The effect of SO_2 concentration in a feed on the catalyst stability was also investigated under the feed composed of 500 ppm NO, 5 vol% O_2 and SO_2 in different ppm levels in N_2. To obtain the kinetic data, the NO conversion was controlled to be less than 10% by adjusting the amount of catalysts and the total flow rate at the same feed composition. The NO_x concentration in the inlet and outlet gas was analyzed by means of an NO/NO_2 combustion gas analyzer (Euroton). From the concentration of the gases at steady state, NO conversion can be calculated according to the following formula:

$$\text{NO conversion } (\%) = \frac{[NO]_{in} - [NO]_{out}}{[NO]_{in}} \times 100$$

The subscripts "in" and "out" indicated the inlet concentration and outlet concentration at steady state, respectively.

RESULTS AND DISCUSSION

The physicochemical properties of supported cobalt oxides are listed in Table 1. We tried to prepare supported cobalt oxides cata-

Table 1. The physicochemical properties of supported cobalt oxides from cobalt nitrate (N) and cobalt acetate (A)

Catalysts	Co content [mmol Co/g]	Surface area [m^2/g]	Specific NO uptake at 298 K [μmol/$g_{cat.}$]
Co_3O_4(A)/CeO_2	1.61	230	503.9
Co_3O_4(N)/CeO_2	1.67	170	32.3
Co_3O_4(A)/ZrO_2	1.59	86	17.4
Co_3O_4(N)/ZrO_2	1.62	90	18.3
CoO_x(A)/SiO_2	1.39	272	47.8
Co_3O_4(N)/SiO_2	1.43	297	2.3

lysts with the same cobalt content. It was determined that each catalyst had the similar cobalt content. The surface area for each catalyst was found to be smaller than that of support itself because some micropores might be plugged during the catalyst preparation. There was no noticeable difference in the surface area between Co_3O_4(N)/ZrO_2 and Co_3O_4(A)/ZrO_2 or between Co_3O_4(N)/SiO_2 and CoO_x(A)/SiO_2. On the other hand, the BET surface area of Co_3O_4(N)/CeO_2 was much smaller than that of Co_3O_4(A)/CeO_2. The specific NO uptake at 298 K was determined for each catalyst and its value decreased in the following order: Co_3O_4(A)/CeO_2>>CoO_x(A)/SiO_2> Co_3O_4(N)/CeO_2>Co_3O_4(N)/ZrO_2~Co_3O_4(A)/ZrO_2>Co_3O_4(N)/SiO_2. The NO uptake appears to be strongly dependent on the supports as well as the cobalt precursors. In the case of zirconia-supported cobalt oxides, the similar NO uptake can be obtained irrespective of kinds of cobalt precursor. On the other hand, the cobalt acetate seems to be beneficial as a cobalt precursor for the larger NO uptake for ceria- and silica-supported cobalt oxides compared with cobalt nitrate.

The effect of cobalt precursor on the catalytic activity for NO oxidation was examined over cobalt oxides supported on SiO_2, ZrO_2 and CeO_2 as shown in Fig. 1. The specific catalytic activity decreased in the following order: Co_3O_4(A)/CeO_2>>CoO_x(A)/SiO_2~Co_3O_4(N)/CeO_2>Co_3O_4(N)/SiO_2>Co_3O_4(N)/ZrO_2>Co_3O_4(A)/ZrO_2. The activation energy was determined to be 64.8, 68.2, 74.0, 93.1, 75.7 and 89.8 kJ/mol for Co_3O_4(A)/CeO_2, CoO_x(A)/SiO_2, Co_3O_4(N)/CeO_2, Co_3O_4(N)/SiO_2, Co_3O_4(N)/ZrO_2 and Co_3O_4(A)/ZrO_2, respectively. CoO_x(A)/SiO_2 showed slightly higher catalytic activity than Co_3O_4(N)/SiO_2 especially at low temperatures. In the case of Co_3O_4/ZrO_2, cobalt oxides prepared from cobalt nitrate showed the higher catalytic activity than cobalt oxides prepared from cobalt acetate. The significant improvement can be found over Co_3O_4/CeO_2 when cobalt acetate was used as a cobalt precursor instead of cobalt nitrate. The close correlation between the specific catalytic activity and the NO uptake at 298 K can be found for all tested catalysts except of Co_3O_4(N)/SiO_2. Co_3O_4(N)/SiO_2 with the least NO uptake at 298 K among tested catalysts showed the higher catalytic activity than Co_3O_4(N)/ZrO_2 and Co_3O_4(A)/ZrO_2.

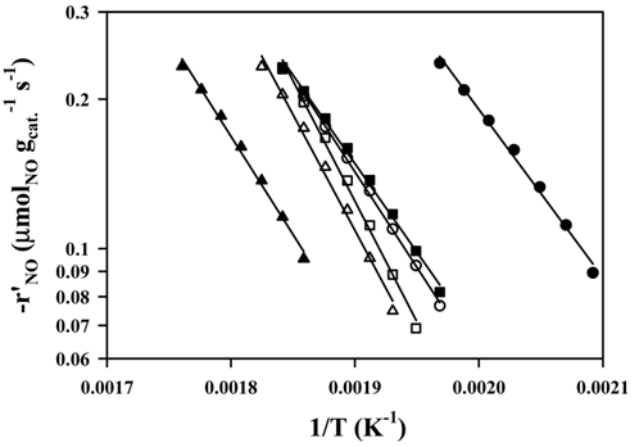

Fig. 1. The specific reaction rate for NO oxidation at different reaction temperatures over supported cobalt oxides from various cobalt precursors: (●) Co_3O_4(A)/CeO_2, (■) CoO_x(A)/SiO_2, (▲) Co_3O_4(A)/ZrO_2, (○) Co_3O_4(N)/CeO_2, (□) Co_3O_4(N)/SiO_2 and (△) Co_3O_4(N)/ZrO_2. Reactants: 500 ppm NO and 5% O_2 in N_2.

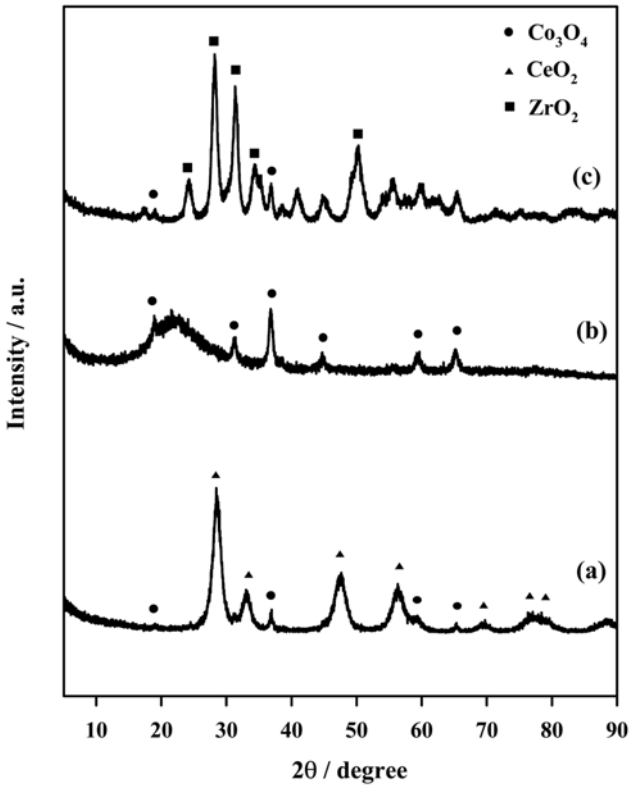

Fig. 2. X-ray diffraction patterns of supported cobalt oxides from cobalt nitrate: (a) Co_3O_4(N)/CeO_2, (b) Co_3O_4 (N)/SiO_2 (c) Co_3O_4(N)/ZrO_2. All catalysts were calcined in air at 573 K before an experiment.

The X-ray diffraction patterns were obtained for all supported cobalt oxides catalysts prepared from cobalt nitrate as a cobalt precursor as shown in Fig. 2. The XRD patterns for supported cobalt oxides catalysts prepared from cobalt acetate have already been presented in our previous work [47]. In all cases, Co_3O_4 was the only observable crystalline structure for cobalt species. No noticeable XRD peak corresponding to Co_3O_4 can be found for CoO_x(A)/SiO_2. On the other hand, the presence of Co_3O_4 can be confirmed for Co_3O_4 (N)/SiO_2. Based on the Scherrer equation, the crystalline size of Co_3O_4 was determined to be 10.3 nm in Co_3O_4(N)/SiO_2. Although the presence of Co_3O_4 phase was confirmed in both Co_3O_4/CeO_2 catalysts, its crystalline size cannot be measured because of its low peak intensity. It can be found that the XRD peak corresponding to Co_3O_4 was stronger for supported cobalt oxides prepared from cobalt nitrate than for supported cobalt oxides prepared from cobalt acetate irrespective of supports used.

To determine the particle size of Co_3O_4 in Co_3O_4(A)/CeO_2, TEM images were obtained as shown in Fig. 3. The finely distributed Co_3O_4 particles can be found and the average particle size was determined to be 3.0±0.6 nm.

The interaction between cobalt oxides and support can be probed with a temperature-programmed reduction (TPR) with H_2. The H_2-TPR was conducted for unsupported Co_3O_4 and cobalt oxides supported on various supports as shown in Fig. 4. For unsupported Co_3O_4,

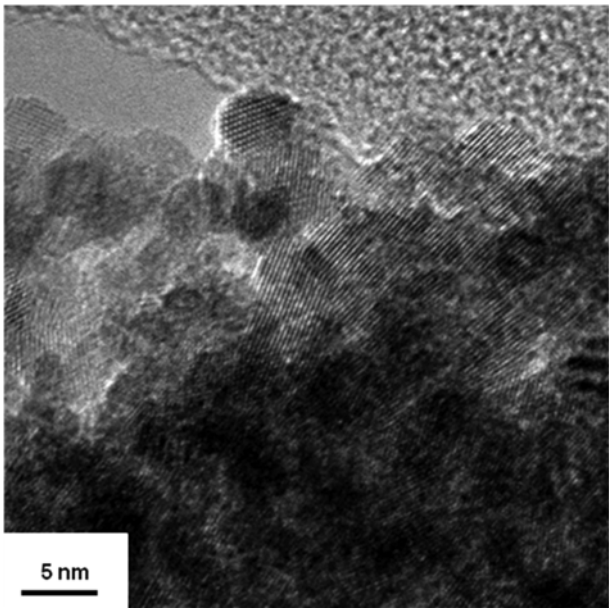

Fig. 3. The bright-field TEM image for Co_3O_4(A)/CeO_2.

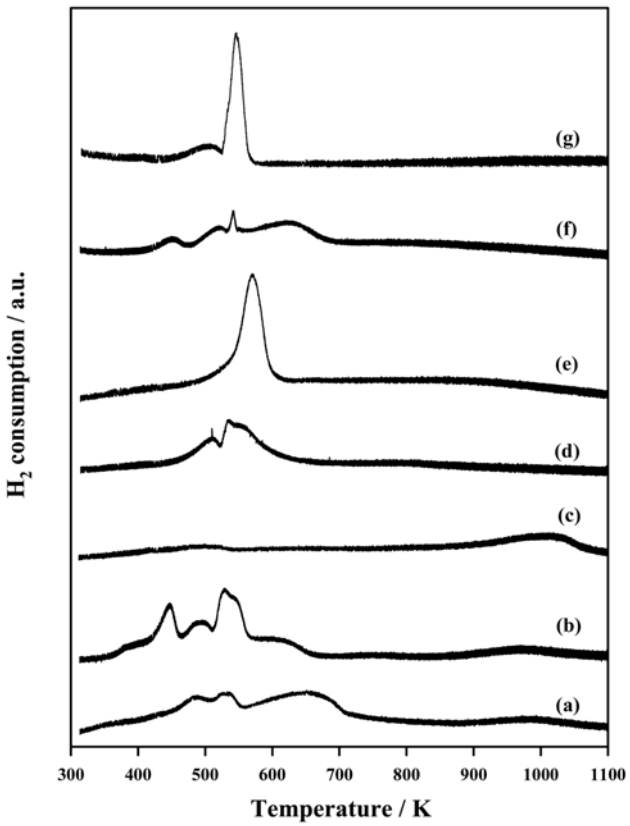

Fig. 4. Temperature programmed reduction (TPR) patterns of supported cobalt oxides from different cobalt precursors: (a) Co_3O_4(A)/CeO_2, (b) Co_3O_4(N)/CeO_2, (c) CoO_x(A)/SiO_2, (d) Co_3O_4(N)/SiO_2 (e) Co_3O_4(A)/ZrO_2, (f) Co_3O_4(N)/ZrO_2, (g) Co_3O_4. All catalysts were calcined in air at 573 K before an experiment.

two reduction peaks with maxima at 502 and 546 K were obtained. These peaks can be due to the sequential reduction of Co_3O_4 into Co through CoO. The TPR peak position can be shifted to the lower temperature with decreasing the crystalline size and also can be moved to the higher temperature with increasing interaction with a support. The similar TPR patterns with that of unsupported Co_3O_4 were obtained for Co_3O_4(N)/SiO_2, which implies that cobalt oxides with the similar reducibility are present in both catalysts. This is consistent with the XRD data supporting that Co_3O_4 is the main crystalline phase of cobalt species in Co_3O_4(N)/SiO_2. However, no TPR peak can be found over CoO_x(A)/SiO_2 at low temperatures, which supports the absence of separate Co_3O_4 crystallites for CoO_x(A)/SiO_2. A high-temperature TPR peak can be observed at 1,016 K for this catalyst. The presence of TPR peak at high temperatures observed in cobalt oxides supported on SiO_2 can be due to the formation of new solid solution phase (e.g., cobalt hydrosilicates [50-52]) which is hardly reducible at low temperatures. A single TPR peak with a maximum at 570 K was observed over Co_3O_4(A)/ZrO_2. On the other hand, several TPR peaks can be obtained over Co_3O_4(N)/ZrO_2. The TPR peak was observed at a lower temperature over Co_3O_4(N)/ZrO_2 than over Co_3O_4(A)/ZrO_2. Compared with other supported cobalt oxides, Co_3O_4/CeO_2 showed the TPR peak at the lowest temperature. The broad TPR peak around 1,000 K can be due to the reduction of bulk CeO_2 into Ce_2O_3 [53]. In the case of CeO_2-supported cobalt oxides, the amount of consumed H_2 for low-temperature TPR peaks was determined to be larger than the theoretical value calculated based on the assumption that all Co_3O_4 was reduced into Co metal. Therefore, some ceria near Co_3O_4 must be reduced during TPR experiment. For all supported cobalt oxides except CoO_x(A)/SiO_2, the presence of Co_3O_4 crystallites can be confirmed from TPR patterns. The TPR peaks at lower temperature were observed for Co_3O_4(A)/CeO_2, Co_3O_4(N)/CeO_2 and Co_3O_4(N)/ZrO_2 compared with those of unsupported Co_3O_4. The TPR pattern revealed that the more active catalyst showed the TPR peak at the lower temperature except silica-supported cobalt oxides. The higher catalytic activity of Co_3O_4(N)/ZrO_2 even with a larger average crystallite size of Co_3O_4 determined from XRD data compared with Co_3O_4(A)/ZrO_2 can be explained by the presence of easily reducible Co_3O_4 determined in H_2-TPR pattern. As mentioned previously, the TPR peak at lower temperature implies the presence of smaller size of Co_3O_4. XRD can give us the bulk structure. Therefore, the finely dispersed clusters with small population may not be detected with a conventional XRD technique. For SiO_2-supported cobalt oxides, it was reported that the kinds of cobalt precursor could affect the pH of the solution in the impregnation step, which resulted in the change of the degree of formation of cobalt silicates detected at high temperatures in the TPR pattern [51]. Therefore, most cobalt species were present as Co_3O_4 in Co_3O_4(N)/SiO_2 prepared from cobalt nitrate, whereas cobalt silicates must be dominant species in CoO_x(A)/SiO_2 prepared from cobalt acetate. The highly dispersed cobalt silicates showed the comparable specific catalytic activity with the crystalline Co_3O_4 on SiO_2.

The effect of H_2O in a feed on the catalytic activity over Co_3O_4(A)/CeO_2 was examined as shown in Fig 5. In the presence of 5 vol% H_2O, the NO conversion decreased compared with the case in the absence of H_2O. The continuous deactivation was also observed with time on stream in the presence of H_2O. However, the fresh activity could be restored after the supply of H_2O in a feed ceased. Therefore, we can say that the catalytic activity for NO oxidation

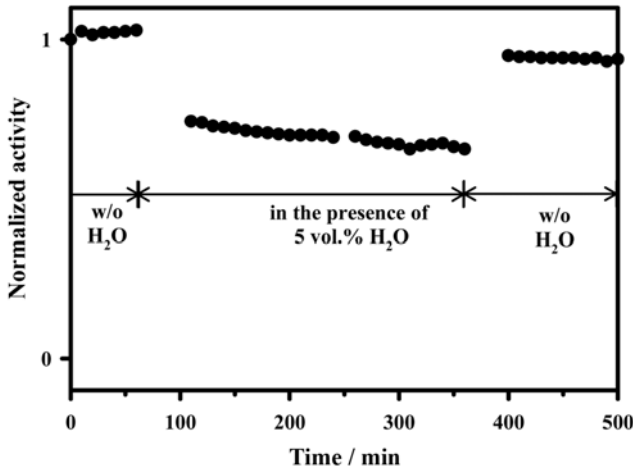

Fig. 5. The normalized activity at 543 K with time on stream over Co_3O_4(A)/CeO_2 containing 1.61 mmol Co/$g_{cat.}$ under different feed composition. This normalized activity was calculated by divining the NO conversion in the presence of H_2O with the NO conversion in the absence of H_2O. 0.15 g of catalyst was contacted with the reactant gas with a total flow rate of 200 ml/min. Common reactants: 500 ppm NO and 5 % O_2 in N_2.

is deactivated reversibly over Co_3O_4(A)/CeO_2 by the presence of H_2O. On the other hand, strong deactivation phenomena were observed in the presence of 100 ppm SO_2 as reported in our previous work [47]. The initial NO conversion could not be restored even after the supply of SO_2 in a feed ceased. Therefore, we can say that the catalytic activity for NO oxidation is deactivated irreversibly in the presence of SO_2. The NO uptake at 298 K was measured for Co_3O_4(A)/CeO_2 after a reaction in the presence of 100 ppm SO_2 and its value was determined to be 51.7 μmol NO/$g_{cat.}$, which is far much

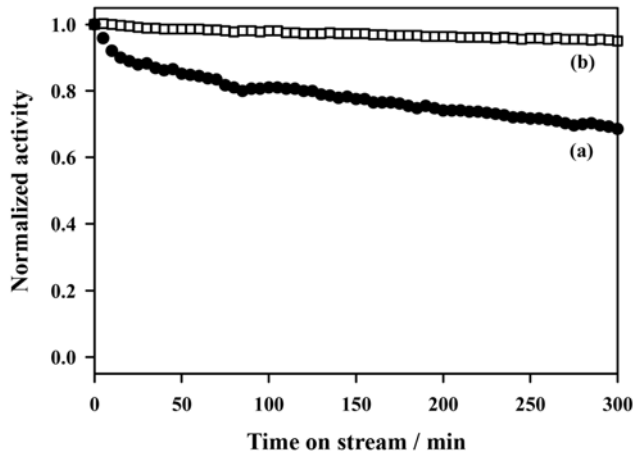

Fig. 6. The normalized activity at 543 K with time on stream over 1 wt% Pt/Al_2O_3 (a) and Co_3O_4(A)/CeO_2 containing 1.61 mmol Co/$g_{cat.}$ (b) in the presence of 5 ppm SO_2. This normalized activity was calculated by divining the NO conversion in the presence of SO_2 with the NO conversion in the absence of SO_2. Reactants: 500 ppm NO, 5 ppm SO_2, 5% O_2 in N_2. 0.15 g of catalyst was contacted with the reactant gas with a total flow rate of 200 ml/min.

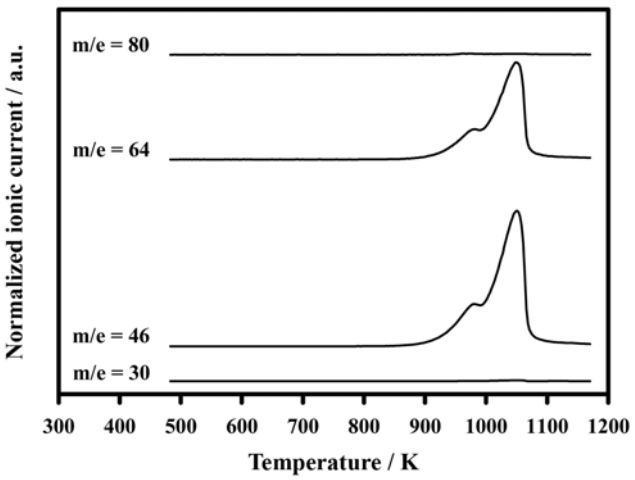

Fig. 7. Temperature programmed oxidation (TPO) patterns for Co_3O_4(A)/CeO_2 after SO_2 poisoning.

smaller than that obtained for the fresh catalyst. This result implies that the adsorption sites for NO can be blocked by SO_2 in a feed. Because the deactivation phenomena can be affected by the concentration of SO_2 in a feed, the catalytic performance was also examined over 1 wt% Pt/Al_2O_3 and Co_3O_4(A)/CeO_2 in the presence of 5 ppm SO_2 in a feed as shown in Fig. 6. Although both catalysts were deactivated even in the presence of 5 ppm SO_2, Co_3O_4(A)/CeO_2 appeared to be more resistant to SO_2 poisoning compared with 1 wt% Pt/Al_2O_3.

The temperature programmed oxidation (TPO) was carried out to find the cause of deactivation due to SO_2 over Co_3O_4(A)/CeO_2 as shown in Fig. 7. NO or SO_3 did not desorb during the TPO experiment. Instead, NO_2 and SO_2 were evolved simultaneously at high temperatures which were far higher than the temperature for NO oxidation in the absence of SO_2 in a feed. These results imply that SO_2 just adsorb on the same sites for NO adsorption and also inhibit desorption of formed NO_2.

CONCLUSIONS

The catalytic activity for NO oxidation over supported cobalt oxides catalysts was affected by the kinds of support as well as the cobalt precursor. The specific catalytic activity decreased in the following order: Co_3O_4(A)/CeO_2>>CoO_x(A)/SiO_2~Co_3O_4(N)/CeO_2>Co_3O_4(N)/SiO_2>Co_3O_4(N)/ZrO_2>Co_3O_4(A)/ZrO_2. This catalytic activity is in line with the specific NO uptake at 298 K except for Co_3O_4(N)/SiO_2. Reversible deactivation was observed over Co_3O_4/CeO_2 in the presence of H_2O. On the other hand, irreversible deactivation occurred over the same catalyst even in the presence of 5 ppm SO_2 in a feed. The strongly adsorbed SO_2 can prohibit NO from adsorbing on the active sites and also can prevent formed NO_2 from desorbing off the catalyst surface. The formation of SO_3 cannot be observed from the chemisorbed SO_2 on Co_3O_4/CeO_2 during TPO.

ACKNOWLEDGMENT

This work was supported by Priority Research Centers Program through the National Research Foundation of Korea (NRF) funded by

the Ministry of Education, Science and Technology (2009-0094047).

REFERENCES

1. A. Fritz and V. Pitchon, *Appl. Catal. B: Environ.*, **13**, 1 (1997).
2. Y. U. Murzin, *Acc. Chem. Res.*, **39**, 273 (2006).
3. B. A. A. L. van Setten, M. Makkee and J. A. Moulijn, *Catal. Rev.-Sci. Eng.*, **43**, 489 (2001).
4. M. A. Gómez-García, V. Pitchon and A. Kiennemann, *Envir. Inter.*, **31**, 445 (2005).
5. Z. Liu and S. I. Woo, *Catal. Rev.- Sci. Eng.*, **48**, 43 (2006).
6. M. Koebel, G. Madia and M. Elsener, *Catal. Today*, **73**, 239 (2002).
7. A. Wokaun, *Ind. Eng. Chem. Res.*, **41**, 4008 (2002).
8. G. Madia, M. Kebel, M. Elsener and A. Wokaun, *Ind. Eng. Chem. Res.*, **41**, 3512 (2002).
9. M. Koebel, M. Elsener and M. Kleemann, *Catal. Today*, **59**, 335 (2000).
10. M. Kang, D. J. Kim, E. D. Park, J. M. Kim, J. E. Yie, S. H. Kim, L. Hope-Weeks and E. M. Eyring, *Appl. Catal. B: Environ.*, **68**, 21 (2006).
11. M. D. Amiridis, T. Zhang and R. J. Farrauto, *Appl. Catal. B: Environ.*, **10**, 203 (1996).
12. M. J. Castagnola, M. K. Neylon and C. L. Marshall, *Catal. Today*, **96**, 61 (2004).
13. J. R. Regalbuto, T. Zheng and J. T. Miller, *Catal. Today*, **54**, 495 (1999).
14. F. C. Meunier and J. R. H. Ross, *Appl. Catal. B: Environ.*, **24**, 23 (2000).
15. J. O. Petunchi and W. K. Hall, *Appl. Catal. B: Environ.*, **2**, L17 (1993).
16. A. Yu. Stakheev, C. W. Lee, S. J. Park and P. J. Chong, *Catal. Lett.*, **38**, 271 (1996).
17. A. Yu. Stakheev, C. W. Lee, S. J. Park and P. J. Chong, *Appl. Catal. B: Environ.*, **9**, 65 (1996).
18. P. W. Park, C. S. Ragle, C. L. Boyer, M. L. Balmer, M. Engelhard and D. McCready, *J. Catal.*, **210**, 97 (2002).
19. H. Ohtsuka, *Appl. Catal. B: Environ.*, **33**, 325 (2001).
20. F. Jayat, C. Lembacher, U. Schubert and J. A. Martens, *Appl. Catal. B: Envirion.*, **21**, 221 (1999).
21. L. Olsson, B. Westerberg, H. Persson, E. Fridell, M. Skoglundh and B. Andersson, *J. Phys. Chem. B*, **103**, 10433 (1999).
22. J. Després, M. Elsener, M. Koebel, O. Kröcher, B. Schnyder and A. Wokaun, *Appl. Catal. B: Environ.*, **50**, 73 (2004).
23. J. Dawody, M. Skoglundh and E. Fridell, *J. Mol. Catal. A*, **209**, 215 (2004).
24. M. Crocoll, S. Kureti and W. Wisweiler, *J. Catal.*, **229**, 480 (2005).
25. Y. Ji, T. J. Toops, U. M. Graham, G. Jacobs and M. Crocker, *Catal. Lett.*, **1-2**, 29 (2006).
26. P. J. Schmitz, R. J. Kudla, A. R. Drews, A. E. Chen, C. K. Lowe-Ma, R. W. McCave, W. F. Schneider and C. T. Goralski Jr., *Appl. Catal. B: Environ.*, **67**, 246 (2006).
27. M. F. Irfan, J. H. Goo, S. D. Kim and S. C. Hong, *Chemosphere*, **66**, 54 (2007).
28. L. Olsson and E. Fridell, *J. Catal.*, **210**, 340 (2002).
29. R. Marques, P. Darcy, P. D. Costa, H. Mellottée, J. M. Trichard and G. Djéra-Mariadassou, *J. Mol. Catal. A*, **221**, 127 (2004).
30. E. Xue, K. Seshan and J. R. H. Ross, *Appl. Catal. B: Environ.*, **11**, 65 (1996).
31. E. Xue, K. Seshan and J. G. van Ommen, *Appl. Catal. B: Environ.*, **2**, 183 (1993).
32. S. S. Mulla, N. Chen, L. Cumaranatunge, G. E. Blau, D. Y. Zemlyanov, W. N. Delgass, W. W. Epling and F. H. Ribeiro, *J. Catal.*, **241**, 389 (2006).
33. L. Li, L. Qu, J. Cheng, J. Li and Z. Hao, *Appl. Catal. B: Environ.*, **88**, 224 (2009).
34. S. Bennici and A. Gervasini, *Appl. Catal. B: Environ.*, **62**, 336 (2006).
35. S. Suárez, S. M. Jung, P. Avila, P. Grange and J. Blanco, *Catal. Today*, **75**, 331 (2002).
36. N. Bogdanchikova, F. C. Meunier, M. Avalos-Borja, J. P. Breen and A. Pestryakov, *Appl. Catal. B: Environ.*, **36**, 287 (2002).
37. E. Kikuchi and K. Yogo, *Catal. Today*, **22**, 73 (1994).
38. R. Brosius, D. Habermacher, J. A. Martens, L. Vradman, M. Herskowitz, L. Čapek, Z. Sobalík, J. Dědeček, B. Wichterlová, Tokarová and O. Gonsiorová, *Top. Catal.*, **30-31**, 333 (2004).
39. L. Čapek, L. Vradman, P. Sazama, M. Herskowitz, B. Wicherlov, R. Zukerman, R. Brosius and J. A. Martens, *Appl. Catal. B: Environ.*, **70**, 53 (2007).
40. J. Y. Yan, H. H. Kung, W. M. H. Sachtler and M. C. Kung, *J. Catal.*, **175**, 294 (1998).
41. G. Bagnasco, M. Turco, C. Resini, T. Montanari, M. Bevilacqua and G. Busca, *J. Catal.*, **225**, 536 (2004).
42. C. Resini, T. Montanari, L. Nappi, G. Bagnasco, M. Turco, G. Busca, F. Bregani, M. Notaro and Rocchini, *J. Catal.*, **214**, 179 (2003).
43. M. M. Yung, E. M. Holmgreen and U. S. Ozkan, *J. Catal.*, **247**, 356 (2007).
44. Q. Wang, S. Y. Park, J. S. Choi and J. S. Chung, *Appl. Catal. B: Environ.*, **79**, 101 (2008).
45. Q. Wang, S. Y. Park, L. Duan and J. S. Chung, *Appl. Catal. B: Environ.*, **85**, 10 (2008).
46. M. F. Irfan, J. H. Goo and S. D. Kim, *Appl. Catal. B: Environ.*, **78**, 267 (2008).
47. D. S. Kim, Y. H. Kim, E. D. Park and J. E. Yie, *Korean J. Chem. Eng.*, **27**(1), 49 (2010).
48. G. Bergeret and P. Gallezot, in *Handbook of Heterogeneous Catalysis*, G. Ertl, H. Knozinger and J. Weitkamp Eds., 446-450, VCH, New York (1997).
49. P. Arnoldy and J. A. Moulijn, *J. Catal.*, **93**, 38 (1985).
50. M. P. Rosynek and C. A. Polansky, *Appl. Catal.*, **73**, 97 (1991).
51. E. van Steen, G. S. Sewell, R. A. Makhothe, C. Micklethwaite, H. Manstein, M. de Lange and C. T. O'Connor, *J. Catal.*, **162**, 220 (1996).
52. Y. Liu, Y. Zhang and N. Tsubaki, *Catal. Commun.*, **8**, 773 (2007).
53. H. C. Yao and Y. F. Yu Yao, *J. Catal.*, **86**, 254 (1984).